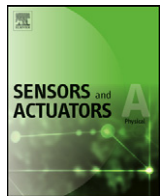




Contents lists available at [SciVerse ScienceDirect](#)

Sensors and Actuators A: Physical

journal homepage: www.elsevier.com/locate/sna



Compensation of drifts in high-Q MEMS gyroscopes using temperature self-sensing

Igor P. Prikhodko*, Alexander A. Trusov, Andrei M. Shkel

MicroSystems Laboratory, Department of Mechanical and Aerospace Engineering, University of California, Irvine, CA, USA

ARTICLE INFO

Article history:

Received 26 August 2012

Received in revised form

15 December 2012

Accepted 17 December 2012

Available online xxx

Keywords:

MEMS gyroscope

Natural frequency

Temperature compensation

Bias drift

Self-sensing

Quality factor

Gyrocompassing

ABSTRACT

We present a long-term bias drift compensation algorithm for high quality factor (Q -factor) MEMS rate gyroscopes using real-time temperature self-sensing. This approach takes advantage of linear temperature dependence of the drive-mode resonant frequency for self-compensation of temperature-induced output drifts. The approach was validated using a vacuum packaged silicon Quadruple Mass Gyroscope (QMG), with signal-to-noise ratio (SNR) enhanced by isotopic Q -factors of 1.2 million. Owing to the high Q -factors, measured frequency resolution of 0.01 ppm provided a temperature self-sensing precision of 0.0004 °C, on par with the state-of-the-art MEMS resonant thermometers. The real-time self-compensation yielded a total bias error of 2°/h and a scale-factor error of 700 ppm over temperature range of 25–55 °C. The presented approach enabled repeatable long-term rate measurements required for MEMS gyrocompassing applications with a milliradian azimuth precision.

© 2013 Elsevier B.V. All rights reserved.

1. Introduction

In recent years several groups have reported silicon MEMS gyroscopes with sub-degree per hour Allan deviation of bias [1–3]. However, long-term bias and scale-factor drifts limit their potential in real-world missions. A major drift source for most MEMS is their inherent sensitivity to temperature variations. An uncompensated bias sensitivity on the order of 500(°/h)/°C is typical for MEMS gyroscopes [4]. Quartz and silicon MEMS resonators used in timing applications exhibit orders of magnitude better long-term stability, due to the more advanced compensation techniques [5]. For instance, high-stability dual-mode oscillators use a secondary mode as a thermometer for the compensation of primary mode drifts [6]. In contrast, conventional approaches for gyroscope calibration rely on third-order thermal models and external temperature sensors, which suffer from the thermal lag and temperature-induced hysteresis [7]. These limitations motivate the development of new real-time self-calibration methods for the inertial MEMS.

Fused quartz Hemispherical Resonator Gyroscope (HRG) utilizes a temperature compensation technique which uses the drive-mode resonant frequency as a measure of gyroscope temperature [8,9]. Successful implementation of this self-sensing technique relies on

two main factors. The first is linearity of the temperature-frequency dependence of the resonator material over wide temperature range; the second is high frequency resolution, brought forth by a high Q -factor. Recently, we introduced a MEMS Quadruple Mass Gyroscope (QMG) [2,3,10], which satisfies these requirements with Q -factor above 1 million, and linear Temperature Coefficient of Frequency (TCF), thanks to the single crystalline silicon resonator body.

The frequency-based measurements of temperature provide inherently better stability than the amplitude-based (analog voltage) readings commonly employed in temperature sensors. For instance, 1 ppm stability and repeatability is easy in the frequency domain, but almost impossible in the analog signal domain [11]. This makes high-resolution temperature self-sensing an intriguing possibility in silicon MEMS technology. Recently, a resonant MEMS thermometer was demonstrated for temperature compensation of a co-fabricated pressure sensor [12]. In this paper, we demonstrate that the resonant temperature self-sensing (Fig. 1) can be used in real-time for the high- Q MEMS gyroscopes to yield a sub-degree per hour total bias error over temperature variations. We present a more complete account of the self-compensation method, originally proposed in [13], and experimentally demonstrate its feasibility over a wider temperature range. We also show that the long-term stability provided by the self-compensation approach allows for repeatable measurements of small angular rates on the order of the Earth's rate, as required for gyrocompassing.

Section 2 presents analysis of temperature-induced drift sources in high- Q gyroscopes. Section 3 describes the temperature

* Corresponding author. Tel.: +1 9498246314.

E-mail address: igor.prikhodko@gmail.com (I.P. Prikhodko).

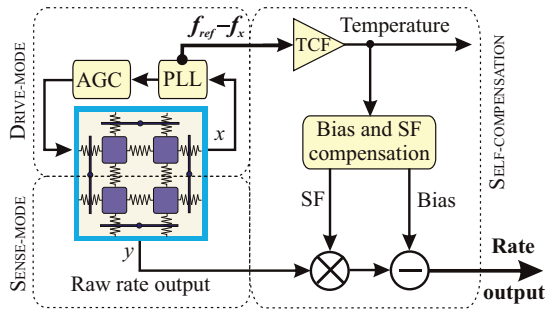


Fig. 1. Signal processing using drive-mode frequency for self-compensation of temperature-induced bias and scale-factor drifts.

self-compensation method and demonstrate its accuracy and precision. Feasibility of a frequency-based temperature self-sensing for bias and scale-factor drifts compensation over temperature is demonstrated in Section 4, followed by conclusions in Section 5.

2. Temperature sensitivity analysis

In this section we analyze temperature-induced drift sources in Coriolis gyroscopes and show the importance of temperature compensation.

2.1. Temperature-induced drifts

Operation of the vibratory z-axis angular rate gyroscopes is based on energy transfer between two vibratory modes, Fig. 2. The drive-mode is continuously excited at resonance, and the sense-mode is used for the rate detection. The amplitude (y) of the sense-mode is proportional to the angular rate along z-axis (Ω_z), with scale-factor (SF) and bias (B):

$$y = (SF) \times (\Omega_z + B). \quad (1)$$

Assuming the worst-case scenario, the sense-mode is operated open-loop, and thus it is more susceptible to temperature variations. Scale-factor and bias are functions of the angular gain ($k \leq 1$), the sense-mode natural frequency ω_y , and the drive amplitude (x) [14]:

$$SF = \frac{2kQ_{\text{eff}}x}{\omega_y}, \quad B = \frac{\Delta(1/\tau) \sin(2\theta_\tau)}{2}, \quad (2)$$

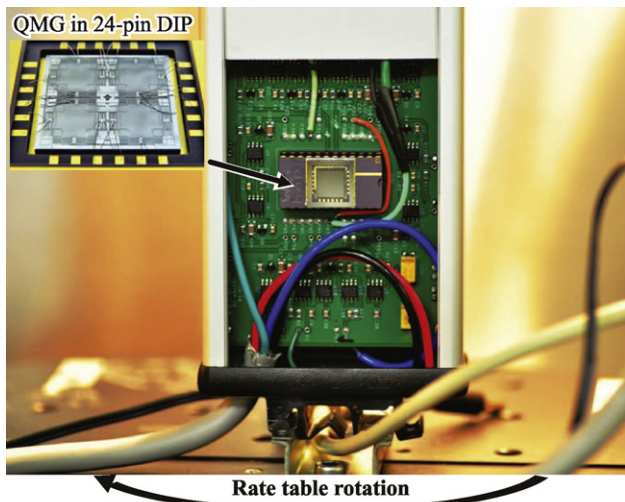


Fig. 2. Photo of the experimental setup, showing the vacuum packaged QMG rate sensor, PCB electronics, and a rate table.

where $\Delta(1/\tau)$ is the damping mismatch between vibratory modes, θ_τ is the principal axis of damping, and Q_{eff} is the effective Q-factor:

$$Q_{\text{eff}} = \frac{Q_y}{\sqrt{1 + 4Q_y^2(\Delta\omega/\omega_y)^2}}, \quad (3)$$

which reaches maximum Q_y at zero frequency mismatch ($\Delta\omega = 0$).

It follows from Eqs. (2) and (3) that the mode-matched condition over wide temperature range, i.e. $\Delta\omega = 0$ and $\Delta(1/\tau) = 0$, is desired to ensure stability of scale-factor and bias. While these requirements can be satisfied by a symmetric transducer design, the temperature dependence of the rest of the parameters (Q_y , ω_y , θ_τ) in Eqs. (1)–(3) still reduces the overall accuracy and repeatability of the rate measurements. The only parameters that can be neglected are the drive amplitude x , stabilized by an Automatic Gain Control (AGC), and the angular-gain factor, k , with a sub-ppm/°C stability over temperature [8]. Thus, the parameter with the highest sensitivity to temperature is either the sense-mode frequency, ω_y , or the sense-mode quality factor, Q_y . Typical temperature sensitivity of the resonant frequency for silicon MEMS is $-31 \text{ ppm/}^\circ\text{C}$ at near room temperature [15]. At the same time, the sensitivity of Q-factor depends on the dominant energy loss mechanism. For the thermo-elastic dissipation, with the associated strong $1/T^3$ temperature dependency [16], the Q-factor sensitivity is the primary factor that contributes to the scale-factor fluctuations ($10,000 \text{ ppm/}^\circ\text{C}$).

2.2. Scale-factor and bias sensitivities

In general, the relationship between the scale-factor (as well as bias) and temperature is non-linear for MEMS gyroscopes. However, for silicon MEMS we can consider the change to be linear in the acceptable temperature range [15]. Quantitatively, we can estimate the effect of the Q-factor on scale-factor by taking the derivative of the expression Eq. (2) with respect to temperature. The result is divided by the nominal scale-factor to find the relative change (assuming $\Delta\omega = 0$):

$$\frac{1}{(SF)} \frac{d(SF)}{dT} = \frac{1}{Q_y} \frac{dQ_y}{dT}. \quad (4)$$

Previously we reported experimental temperature characterization of the Q-factor for the vacuum sealed QMG, which confirmed that the dominant energy loss mechanism is the thermoelastic dissipation [2]. Linear fit to the $Q(T)$ data in Fig. 3 reveals dQ_y/dT of $12,000 \text{ }^\circ\text{C}^{-1}$, yielding a scale-factor sensitivity of $10,000 \text{ ppm/}^\circ\text{C}$ at near room temperature. Calculation of the derivatives dQ_y/dT at different temperatures shows that the sensitivity varies from

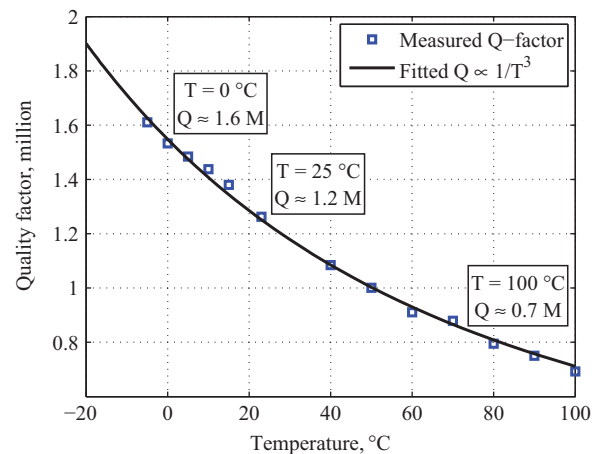


Fig. 3. Measured Q vs. temperature for a packaged QMG. The $1/T^3$ dependence is attributed to the thermoelastic dissipation.

5000 ppm/°C to 20,000 ppm/°C over wider temperature range of –40°C to 120°C.

Temperature sensitivity of bias, Eq. (2), is significantly reduced by the geometric symmetry of a QMG transducer, which ensures damping isotropy $\Delta(1/\tau)$ over wide temperature range. Nevertheless, fabrication and packaging imperfections, as well as electronic components drifts may contribute to change in the angle θ_r of the principal axis of damping, and thus overall temperature sensitivity of the gyroscope bias.

3. Frequency-based temperature self-sensing

In this section we describe the temperature compensation method and demonstrate its accuracy and precision using QMG.

3.1. Resonant temperature sensing for drifts compensation

While the gyroscope drive-mode is controlled by a Phase-Locked Loop (PLL) and an AGC loop, the open-loop sense-mode is susceptible to temperature variations, as shown in the previous section. To compensate for temperature-induced scale-factor and bias drifts, we propose to use the drive-mode frequency as a built-in thermometer, which is free from any spatial or temporal thermal lag. The silicon resonator frequency changes linearly with the temperature, so by monitoring this change, on-chip gyroscope temperature can be measured directly. The temperature coefficient of frequency is well defined by elastic properties and its value is fixed for a given material (e.g. silicon) [15], which allows for repeatable measurements of the temperature.

Fig. 1 shows signal processing for the real-time self-compensation of both scale-factor and bias drifts. The instantaneous frequency change is first correlated to the temperature using the measured TCF. Once the instantaneous temperature value is obtained, it is used to estimate (predict) the scale-factor and bias drifts in real-time. Finally, the raw gyroscope output is corrected by multiplying it with the scale-factor change, followed by subtraction of bias drifts.

The gyroscope bias can be modeled as a constant (bias offset) plus a time-varying component (bias drift), which is primarily caused by the temperature fluctuations. For the first-order temperature T compensation, bias b is approximated by the sum of the offset value b_{T_0} and a linear term with the coefficient β_T :

$$b(T) = b_{T_0} + \beta_T \Delta T, \quad (5)$$

which due to the linear temperature dependence of frequency $f=f(T)$ can be represented in terms of the natural frequency change Δf :

$$b(f) = b_{f_0} + \beta_f \Delta f. \quad (6)$$

The temperature sensitivity coefficient β_f and the constant b_{f_0} are determined through the least-square linear fit to the calibration data, see Section 4.1. The frequency change Δf is used to estimate the temperature-induced bias drift $b(f)$ and perform compensation in real-time. Similarly, self-compensation method is performed for the scale-factor.

3.2. Temperature characterization of transducer

The QMG transducer [17] was chosen for evaluation of the approach due to its symmetric high-Q design and isotropy of both frequency and damping. The QMG architecture comprises four identical tines, four linear coupling flexures, and a pair of lever mechanisms for synchronization of the anti-phase drive- and sense-mode motion. Both momentum and torque balance in both x and y directions are provided by the lever mechanisms and flexures enable ultra-low dissipation of energy through

the substrate, leading to a high resolution and equal high Q -factors, $Q_x = Q_y > 1$ million. At the same time, structural symmetry of the QMG lumped mechanical element provides closely matched drive- and sense-mode TCFs for increased robustness to the temperature-induced drifts as required for high precision rate measurements.

Stand-alone QMGs were fabricated using an SOI process with a 100- μm thick device layer. Singulated devices were vacuum sealed using getters inside a ceramic package, providing sub-mTorr vacuum sustainable over many years. Characterization of the packaged QMGs showed drive- and sense-mode Q -factors of 1.17 million at 25°C and 0.7 million at 100°C, with $\Delta Q/Q$ symmetry of 1%, or $\Delta(1/\tau)$ of 10°/h [2]. Frequency symmetry $\Delta\omega$ over temperature range of 30°C to 75°C was also confirmed with a 0.2 ppm/°C confidence bounds. High Q -factor is expected to provide a sub-ppm frequency stability, required for high-precision frequency-based temperature sensing.

3.3. Temperature self-sensing accuracy and precision

The signal processing for temperature self-sensing takes advantage of the high Q -factors and linear TCF of the silicon QMG. As shown in Fig. 1, a PLL monitors the resonant frequency change relative to the high-stability frequency reference (0.05 ppb over 30 s) [18], which is then converted to temperature. The stability of the frequency reference is thus critical as it defines the lower bound on the minimum resolvable temperature. Accuracy of the frequency-to-temperature conversion relies on accuracy and linearity of the TCF value. The TCF was measured over a temperature range of 30–75°C using a high precision thermistor from GEC Instruments with accuracy and precision of approximately 10^{–4} °C. The TCF of –24 ppm/°C was calculated from a linear fit to the frequency–temperature data with an accuracy of 0.04 ppm/°C, Fig. 4.

The precision of frequency-based temperature sensing depends on the resonant frequency stability of the anti-phase drive-mode of the gyroscope. Due to high Q -factor, we demonstrated a 40 ppb/ $\sqrt{\text{Hz}}$ white noise of frequency, resulting in 10 ppb frequency resolution at 30 s for the QMG near room temperature [10], Fig. 5. Using the TCF of –24 ppm/°C, the measured frequency stability translates to temperature self-sensing precision of 0.002 °C at 1 s averaging time and 0.0004 °C at 30 s averaging time (with an accuracy of 0.002 °C), on par with the state-of-the-art MEMS resonant thermometers [19–21]. Next, we demonstrate the self-compensation of temperature drifts using the gyroscope as a high-resolution frequency thermometer.

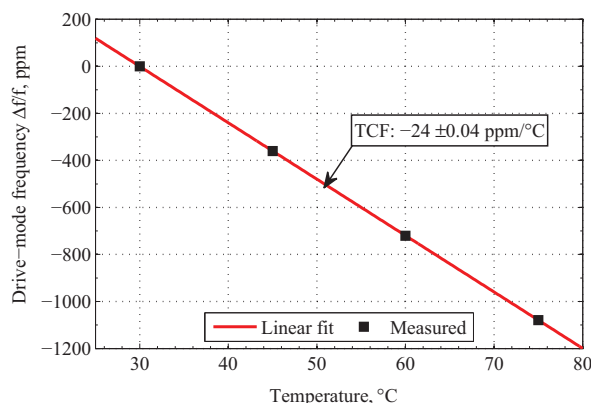


Fig. 4. Linear frequency–temperature dependence, revealing a -24 ± 0.04 ppm/°C TCF over temperature range of 30–75°C.

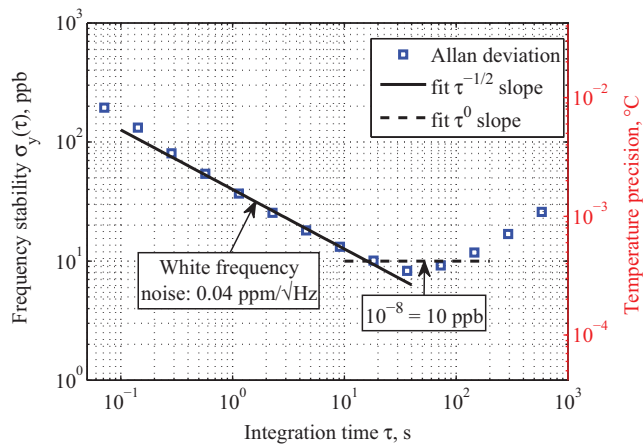


Fig. 5. Experimental demonstration of 10^{-8} frequency stability, which translates to 4×10^{-4} °C precision of temperature self-sensing.

4. Experimental demonstration of self-compensation

Frequency-based temperature self-sensing can be used in various applications. In this work, we demonstrate feasibility of a high resolution frequency thermometer for (i) in-run bias and scale-factor drifts compensation over temperature range, (ii) gyro-compassing error correction over temperature range, and (iii) turn-on bias compensation. For all experiments the gyroscope control shown in Fig. 1 was implemented using a HF2 Zurich Instruments (ZI) hardware. The drive-mode of the QMG was operated closed-loop, while the sense-mode remained open-loop. The PLL-based drive-loop sustained oscillation at resonance and provided reference for the signal demodulations. The AGC stabilized the amplitude of drive-mode motion. The gyroscope output proportional to the angular rate was detected by demodulating the sense-mode signal at 90° phase.

4.1. Calibration run

To determine the model parameters (bias offset b_{f0} and temperature coefficient β_f), we performed a calibration run over a temperature range from 35 °C to 55 °C using a custom-built package-level heater, Fig. 6. These experiments were conducted using the vacuum sealed QMG with a nominal frequency separation of 3.8 Hz between drive- and sense-mode (without frequency tuning or trimming). The temperature range above 35 °C was chosen in order to separate the transducer drifts from the interface electronics drifts, see Section 4.5 for details on cold-start and effects of self-heating. Static calibration at zero input rate doesn't allow to separate the bias drift (null offset drift) from the scale-factor drift. For this reason periodical physical rotations ($\pm 0.5^\circ/\text{s}$) were applied to the gyroscope at different temperatures. Scale-factor estimation in the presence of a constant angular rate (e.g. Earth's rate) is also possible by the input modulation, see Section 4.4 for details.

A linear relationship was observed for the bias drift as a function of the on-chip gyroscope temperature, Fig. 7(a). The temperature values in Fig. 12 were obtained by monitoring the gyroscope drive-mode frequency and using the linear TCF value for the conversion. The linear least squares fit to the experimental data was performed to determine calibration parameters for the linear bias model (Eq. (6)), revealing β_f of approximately $1.5(^\circ/\text{h})/\text{ppm}$ or β_T of $-35(^\circ/\text{h})/^\circ\text{C}$.

The scale-factor sensitivity was determined from the same experiment. A temperature change of approximately 17 °C resulted in a 20% drop of the scale-factor, yielding a temperature coefficient of $-12,000 \text{ ppm}/^\circ\text{C}$ (or 1.2%), in a fairly good agreement with its

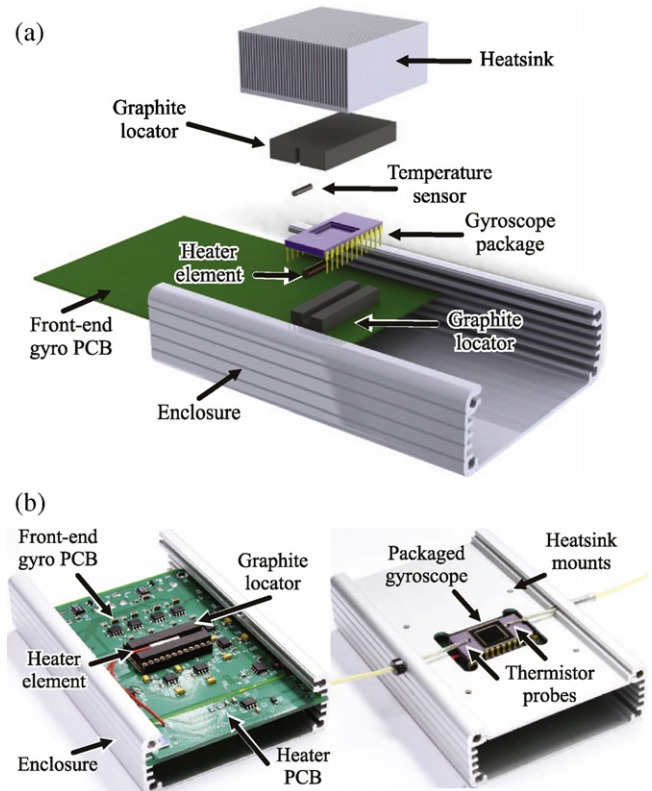


Fig. 6. The custom-built package-level resistive heater assembly for thermal calibration of a gyroscope. (a) Exploded view of the assembly model in Solidworks. (b) Photographs of assembly process showing heater element, gyroscope and temperature sensor locations.

theoretical value of $10,000 \text{ ppm}/^\circ\text{C}$ estimated in Section 2.2. These measured sensitivity coefficients of bias and scale-factor were used to perform self-compensation of the sense-mode drifts according to the signal processing scheme, Fig. 1.

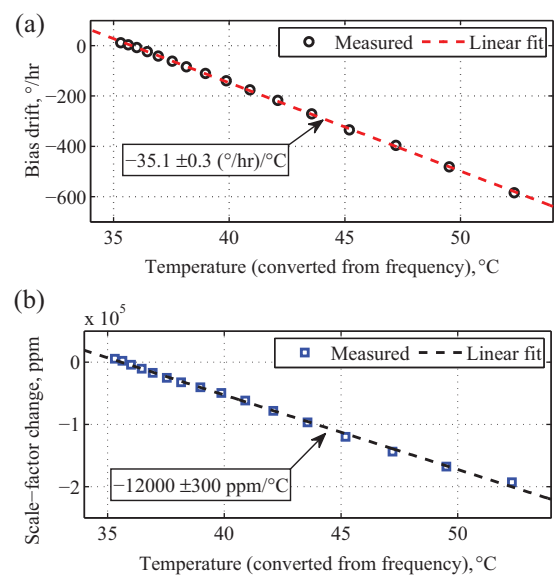


Fig. 7. Calibration run, revealing linear temperature dependences of bias and scale-factor drifts over a temperature range of 35–55 °C. (a) Temperature sensitivity of bias with a coefficient of $-35(^\circ/\text{h})/^\circ\text{C}$. (b) Temperature sensitivity of scale-factor with a coefficient of $1\%/^\circ\text{C}$.

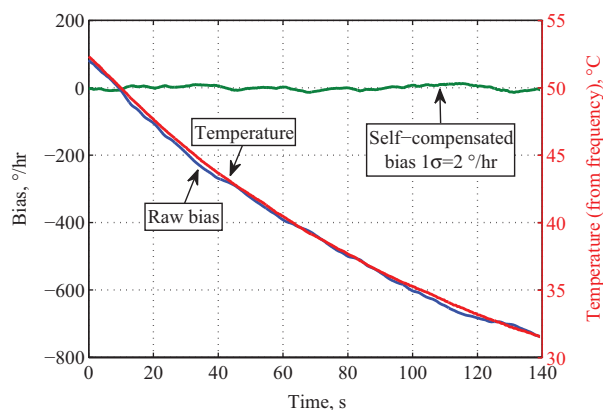


Fig. 8. Time history of a QMG output over a relatively rapid temperature change from approximately 50°C to 30°C. Self-compensation removes temperature-induced drift to below 2°/h (1σ).

4.2. Real-time self-compensation of gyroscope drifts

As discussed in Section 3.2, both frequency and damping symmetry of the QMG significantly reduce scale-factor and bias temperature sensitivities. Nevertheless, imperfections in fabrication, packaging, and electronic component drifts contribute to sensor's temperature sensitivity. To validate the proposed self-compensation method and ensure repeatability of the calibrated model parameters, we monitor raw and self-compensated gyroscope output over temperature changes.

Once the gyroscope was heated up to 55°C the heater was turned off and the output was recorded until the temperature reached 30°C. Fig. 8 shows a time history of the QMG output over a temperature change of approximately 20°C, revealing a strong temperature correlation of the raw bias. The natural frequency obtained in real-time from the PLL was used to estimate and compensate both bias and scale-factor drifts according to the predictive first-order model Eq. (6). The temperature values in Fig. 8 were also derived from the drive-mode frequency. The self-compensation of sense-mode drifts reduced the apparent long-term drift and reduced the temperature correlation from 98% to below the measurement error, indicating that the gyroscope output was no longer affected by the temperature fluctuations. The self-compensation removed temperature-induced drift to below 2°/h standard deviation (1σ) of bias error despite the fast 20°C temperature change.

4.3. Long-term stability analysis

Allan deviation analysis allows determination of random processes present in a gyroscope output. To perform analysis, the gyroscope static measurements (zero rate output and temperature) were recorded for a period up to 24 h at room temperature. During this time interval, the gyroscope on-chip temperature had been varying in a range from 23.7°C to 24.2°C. This temperature change led to the uncompensated bias drift of about 90°/h, Fig. 9. The self-compensation method has been employed to remove temperature drifts to below 0.5°/h standard deviation (1σ) of bias error and resolved additional non-temperature-induced noise processes (e.g. rate random walk).

As discussed earlier, the advantage of the proposed self-sensing method is the absence of thermal lag and hysteresis. Table 1 compares the compensation accomplished by using the proposed self-sensing versus using the high-precision temperature sensor (GEC Instruments) placed in close proximity to the gyroscope. For the long-term stability assessment we compared our rate random walk (RRW) values, Fig. 10. Allan deviation of the raw data (from

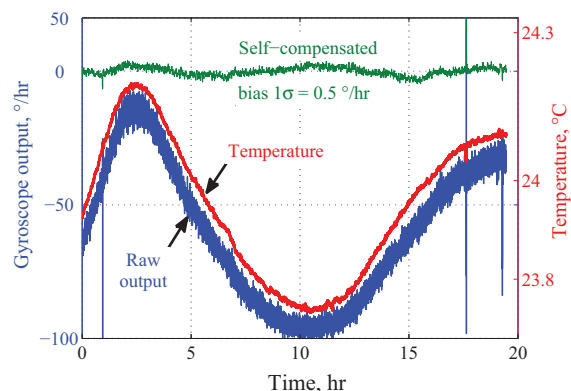


Fig. 9. Time history of a static QMG zero rate output over the room temperature variations. Self-compensation removes temperature-induced drift to below 0.5°/h (1σ).

Table 1

Comparison of drift compensation methods (Fig. 10 data).

| Method | ARW °/√h | Bias stability °/h | Time Constant min | RRW °/h/√h |
|--------------------|-------------|-----------------------|----------------------|---------------|
| Uncompensated | 0.1 | 0.6 | 3 | – |
| Temperature sensor | 0.1 | 0.35 | 10 | 1 |
| Self-sensing | 0.07 | 0.22 | 20 | 0.3 |

Fig. 9) revealed the bias instability of 0.6°/h after $\tau = 3$ min integration time. For longer integration times the output was dominated by the temperature ramp with a τ^{+1} slope.

The bias drift compensation using the external thermistor resolved RRW process of 1°/h/√h, showing that the temperature ramp was removed. Despite an excellent thermistor accuracy, conventional compensation did not significantly improve the bias instability due to apparent thermal lag. In contrast, self-compensation resulted in a threefold improvement of the bias instability, providing a 0.2°/h value at 20 min. Most importantly, the RRW improved down to 0.3°/h/√h, indicating long-term stability. Next, we used gyrocompassing application to illustrate the advantages of self-compensation for improving repeatability.

4.4. Self-compensation for gyrocompassing

One of the demanding inertial applications that require long-term stability is gyrocompassing for non-magnetic north-finding.

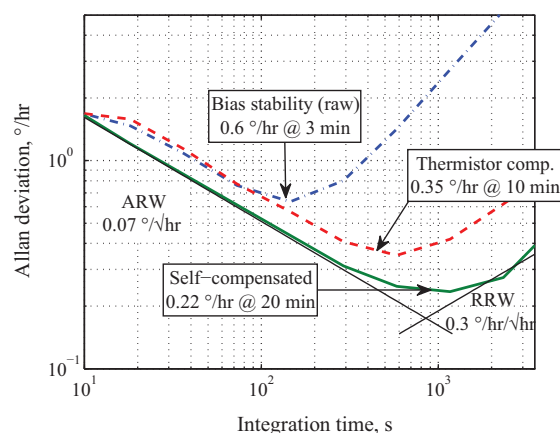


Fig. 10. Allan deviation of gyroscope outputs over temperature variations, showing a 0.2°/h self-compensated bias instability.

While north-finding is discussed in [3], here we highlight effects of temperature-induced drifts.

Gyrocompassing requires constant bias over temperature for repeatable measurements. In practice, however, time-varying bias prevents from the long-term stable measurements of slow angular rates. To experimentally measure drifts, we mounted the QMG with its input axis horizontal relative to a rotary platform and separated scale-factor from the sensor's bias by virtue of continuous rotation in a horizontal plane. The method is similar to the carouseling technique used for continuous modulation of constant rotation rate of the Earth [3]. Demodulation of the output at the frequency of the applied rotation allows to extract bias and scale-factor while performing gyrocompassing (true azimuth) measurements. The experiments were conducted using the vacuum sealed QMG with a frequency separation of 0.16 Hz between the drive- and sense-mode in order to improve sensitivity of the gyroscope (achieved by the electrostatic frequency tuning). The trade-off however is the increased temperature sensitivity of the sense-mode, which requires new calibration parameters.

Fig. 11 shows a QMG output from a carouseling run. The gyro was able to detect the horizontal component of the Earth's rate, approximately 12.51°/h in Irvine, California (33.7°N latitude). The raw data shows a low-frequency temperature-induced drift, which can be removed by self-compensation. The rotation in plane with a 1°/s rate effectively modulated the constant Earth's rate with a 6-min period. Each period (each 360° turn) the data was logged and a sinusoidal fit was performed in real-time to obtain calibration parameters (during which the temperature is assumed to be constant). Every 6 min a new calibration set of bias, scale-factor, and azimuth was obtained and analyzed. The gyroscope bias is an offset value of the fit, the scale-factor is an amplitude of the fit, and the azimuth angle is a phase of this fit. Filtering of the data produced azimuth estimation with uncertainty diminishing as the square root of the number of measurements, reaching a 4 milliradian precision after 100 averages.

From these measurements, a strong correlation between the gyroscope bias and the temperature was observed during a 16-h run, Fig. 12(a). The measured 99% correlation confirmed environmental changes to be the primary drift source. A linear relationship was observed for bias (null offset) as a function of the on-chip gyroscope temperature, Fig. 12(b). The direct gyroscope temperature

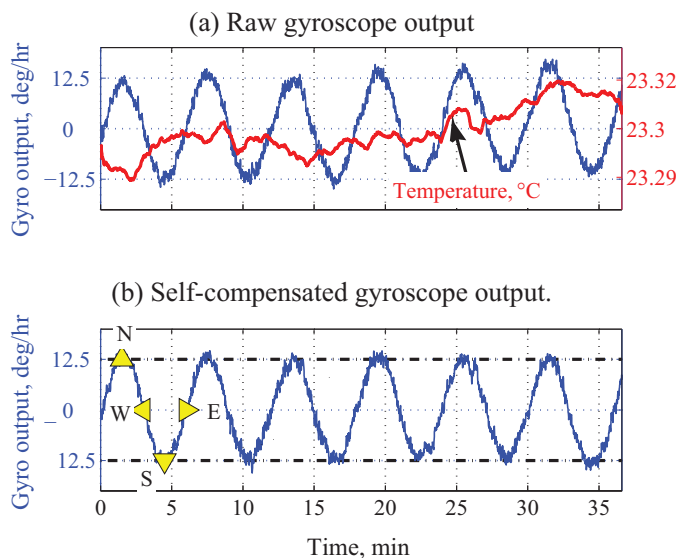


Fig. 11. Earth's rate measurements during gyrocompassing. The gyroscope output is 12.6°/h when pointing North (at Irvine, CA location). Temperature-induced drift is removed after self-compensation.

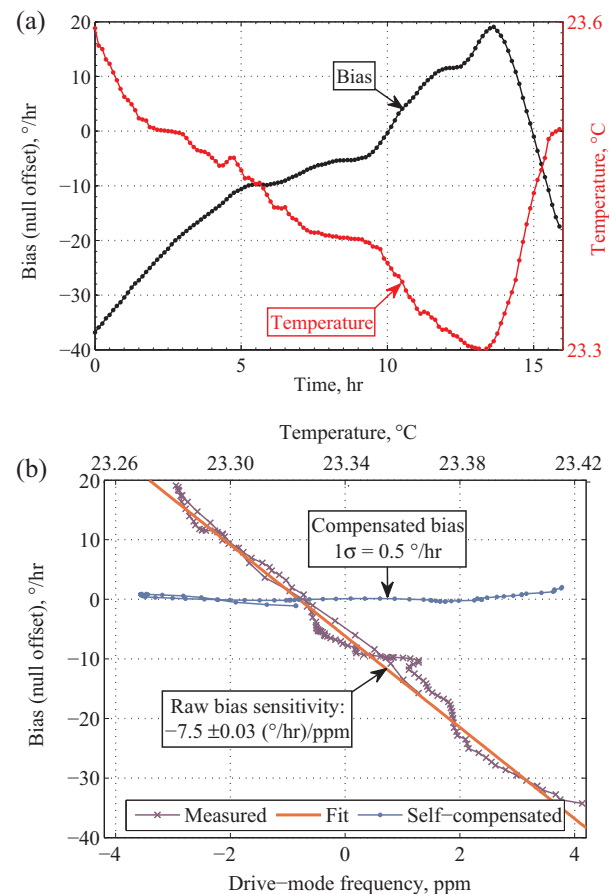


Fig. 12. Raw and self-compensated gyroscope bias during gyrocompassing measurements in room temperature. (a) Experimentally measured 99% temperature correlation of a gyroscope bias during a 16-h run (uncompensated data). (b) Raw and self-compensated gyroscope bias, revealing a 1σ bias total error of 0.5°/h over room temperature variations during 16-h run.

was self-sensed by monitoring its resonant frequency. The temperature sensitivity coefficient of $-7.5 \pm 0.03 (^\circ/\text{h})/\text{ppm}$ was found by the linear least squares fitting, which translates to the bias coefficient of $-180 \pm 0.8 (^\circ/\text{h})/^\circ\text{C}$ (attributed to the packaging stresses in early QMG prototypes). This sensitivity coefficient was used to perform self-compensation of temperature-induced bias drifts near the room temperature. Self-compensation removed the linear trend and enabled a total 1σ bias error of 0.5°/h over day/night temperature variations, Fig. 12(b). As expected, the temperature sensitivity of bias was increased due to reduced frequency separation between the sense- and the drive-modes. Similarly, temperature self-compensation using the gyroscope frequency as a thermometer resulted in a total 1σ scale-factor error of 700 ppm over day/night temperature variations, confirming feasibility of the approach.

4.5. Self-compensation of turn-on bias drift

In this section we demonstrate that the self-heating induced turn-on bias error of the high-Q quadruple mass gyroscope can be reduced by the proposed self-compensation approach. By monitoring the gyroscope natural frequency, this temperature sensitivity can be eliminated.

During the turn-on event the front-end electronics heats up with the temperature gradient across the printed circuit board (PCB), Fig. 13. This in turn leads to the increase in device's temperature. Fig. 14 shows time history of the package and electronics

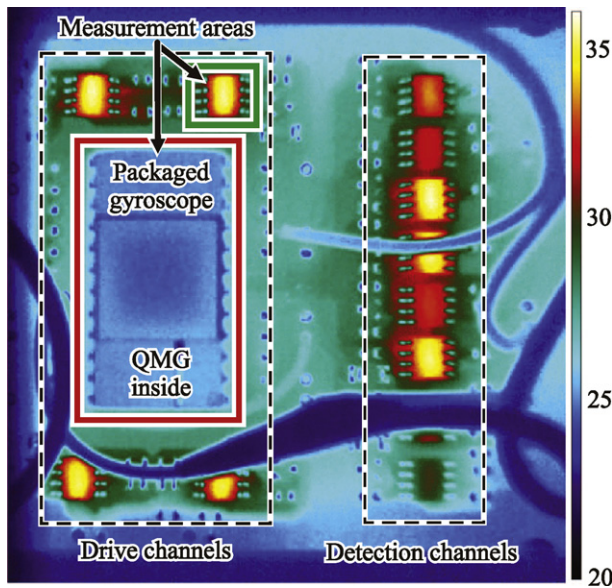


Fig. 13. Infrared image of the PCB circuit, showing temperatures of electronic components and the device's ceramic package. The colorbar shows the temperature in degrees Celsius.

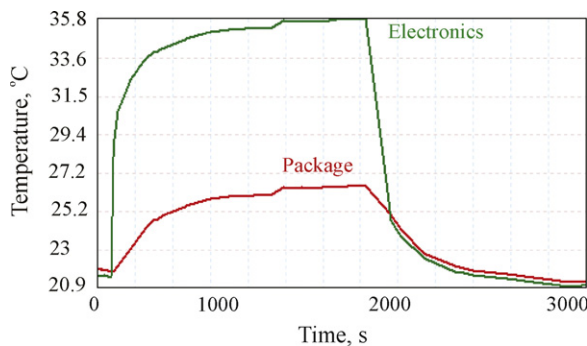


Fig. 14. Time history of temperature for the package and electronics recorded using IR camera (from locations shown in Fig. 13) during PCB power turn-on and turn-off events, revealing self-heating of the device up to about 27 °C.

temperature during the PCB power turn-on and turn-off events, demonstrating a self-heating from 21 °C to 27 °C for the gyroscope's ceramic package. This in turn lead to the bias (offset voltage) drift of 2000°/h (the scale-factor is assumed to be constant throughout the turn-on event).

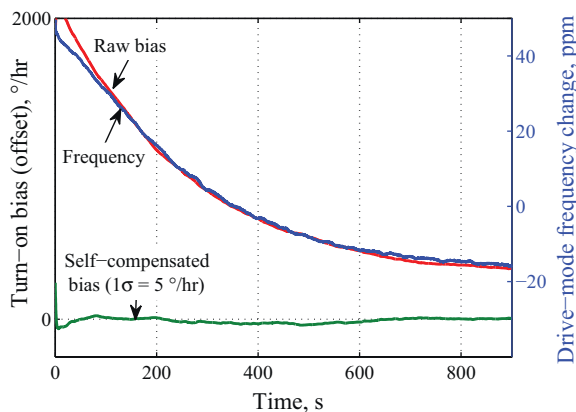


Fig. 15. Self-compensated gyroscope bias, revealing a 1 σ turn-on bias error of 5°/h despite electronics self-heating.

A strong correlation is observed for bias (null offset) as a function of the on-chip gyroscope frequency, Fig. 15. The resonant frequency change is indicative of the gyroscope temperature change as shown previously. Self-compensation removed the linear trend and enabled a total 1 σ bias error of 5°/h during 900 s of temperature ramp-up since the cold-start, proving feasibility of the approach, Fig. 15.

5. Conclusions

We demonstrated the self-compensation of the gyroscope drifts by utilizing its resonant frequency as an embedded thermometer. The approach is based on linear frequency–temperature dependence in the silicon Quadruple Mass Gyroscope, with SNR enhanced by high Q-factor. In contrast to conventional thermal compensation methods (e.g. placing a temperature sensor in close proximity to the gyroscope), the proposed self-sensing approach is inherently independent from a thermal lag, enabling compensation of drifts in real time and eliminating need for additional external sensors. The measured frequency stability of 0.01 ppm provided a temperature self-sensing precision of 0.0004 °C, on par with the state-of-the-art MEMS resonant thermometers. Self-compensation removed the sense-mode temperature sensitivity and improved the Allan deviation of bias from 0.6 to 0.2°/h. Most importantly, this method enabled a total bias error of 2°/h in run and a total scale-factor error of 700 ppm over temperature variations. The demonstrated self-compensation method may provide a path for inertial-grade silicon MEMS gyroscopes with long-term bias and scale-factor stability.

Acknowledgements

This material is based upon work supported by the ONR/NSWCDD and DARPA/SPAWAR under grants N00014-09-1-0424, N00014-11-1-0483, and N66001-12-C-4035. The authors thank Dr. S. Zotov from UC Irvine, I. Chepurko from Mistras Group Inc., and Dr. F. Heer from Zurich Instruments AG for assistance with the front-end electronics.

References

- [1] F. Ayazi, Multi-DOF inertial MEMS: from gaming to dead reckoning, in: Proceedings of the 16th International Solid-State Sensors, Actuators and Microsystems Conference (Transducers'11), Beijing, China, June 5–9, 2011, pp. 2805–2808.
- [2] I.P. Prikhodko, S.A. Zotov, A.A. Trusov, A.M. Shkel, Sub-degree-per-hour silicon MEMS rate sensor with 1 million Q-factor, in: Proceeding of the 16th International Solid-State Sensors, Actuators and Microsystems Conference (Transducers'11), Beijing, China, June 5–9, 2011, pp. 2809–2812.
- [3] I.P. Prikhodko, A.A. Trusov, A.M. Shkel, North-finding with 0.004 radian precision using a silicon MEMS quadruple mass gyroscope with Q-factor of 1 million, in: Proceedings of the 25th IEEE International Conference on Micro-Electro-Mechanical Systems (MEMS'12), Paris, France, January 29–February 2, 2012, pp. 164–167.
- [4] M. Weinberg, A. Kourepenis, Error sources in in-plane silicon tuning-fork MEMS gyroscopes, IEEE Journal of Microelectromechanical Systems 15 (2006) 479–491.
- [5] R. Melamud, P. Hagelin, C. Arft, C. Grosjean, et al., MEMS enables oscillators with sub-ppm frequency stability and sub-ps jitter, in: Solid-State Sensors, Actuators, and Microsystems Workshop 2012, Hilton Head Island, South Carolina, USA, June 3–7, 2012.
- [6] J.R. Vig, Temperature-insensitive dual-mode resonant sensors – a review, IEEE Sensors Journal 1 (1) (2001) 62–68.
- [7] K. Shcheglov, C. Evans, R. Gutierrez, T.K. Tang, Temperature dependent characteristics of the JPL silicon MEMS gyroscope, in: Proceedings of the IEEE Aerospace Conference, vol. 1, 2000, pp. 403–411.
- [8] D.M. Rozelle, The hemispherical resonator gyro: from wineglass to the planets, in: Proceedings of the 19th AAS/AIAA Space Flight Mechanics Meeting, February, 2009, pp. 1157–1178.
- [9] X. Wang, W. Wu, Z. Fang, B. Luo, Y. Li, Q. Jiang, Temperature drift compensation for hemispherical resonator gyro based on natural frequency, Sensors 12 (5) (2012) 6434–6446.

- [10] S.A. Zotov, A.A. Trusov, A.M. Shkel, High-range angular rate sensor based on mechanical frequency modulation, *IEEE Journal of Microelectromechanical Systems* 21 (2) (2012 Apr) 398–405.
- [11] T.-C. Clark, Nguyen, The harsh environment robust micromechanical technology (HERMiT) program: success and some unfinished business, in: *Proceedings of the IEEE International Microwave Symposium Digest (MTT-S 2012)*, June 17–22, 2012, pp. 1–3.
- [12] C.-F. Chiang, A.B. Graham, E.J. Ng, C.H. Ahn, G.J. O'Brien, T.W. Kenny, A. Novel, High-resolution resonant thermometer used for temperature compensation of a fabricated pressure sensor, in: *Solid-State Sensors, Actuators, and Microsystems Workshop 2012*, Hilton Head Island, South Carolina, USA, June 3–7, 2012.
- [13] I.P. Prikhodko, A.A. Trusov, A.M. Shkel, Achieving long-term bias stability in high-Q inertial MEMS by temperature self-sensing with a 0.5 millikelvin precision, in: *Solid-State Sensors, Actuators, and Microsystems Workshop 2012*, Hilton Head Island, South Carolina, USA, June 3–7, 2012, pp. 287–290.
- [14] D.D. Lynch, Coriolis vibratory gyros, in: *Proceedings of the Symposium on Gyro Technology*, Stuttgart, Germany, 1998, pp. 1.0–1.14 (reproduced as Annex B, Coriolis Vibratory Gyros, pp. 56–66 of IEEE Standard 1431-2004. IEEE Standard Specification Format Guide and Test Procedure of Coriolis Vibratory Gyros, IEEE Aerospace and Electronic Systems Society, 20 December, 2004).
- [15] M.A. Hopcroft, W.D. Nix, T.W. Kenny, What is the Young's modulus of silicon? *IEEE Journal of Microelectromechanical Systems* 19 (2) (2010 Apr) 229–238.
- [16] M.A. Bongsang Kim, R.N. Hopcroft, C.M. Candler, M. Jha, R. Agarwal, S.A. Melamud, G. Yama Chandorkar, T.W. Kenny, Temperature dependence of quality factor in MEMS resonators, *IEEE Journal of Microelectromechanical Systems* 17 (3) (2008 Jun) 755–766.
- [17] A.A. Trusov, I.P. Prikhodko, S.A. Zotov, A.M. Shkel, Low-dissipation silicon MEMS tuning fork gyroscopes for rate and whole angle measurements, *IEEE Sensors Journal* 11 (11) (2011 Nov) 2763–2770.
- [18] HF2 User Manual, Zurich Instruments AG, 2012.
- [19] E.J. Ng, H.K. Lee, C.H. Ahn, R. Melamud, T.W. Kenny, Stability measurements of silicon MEMS resonant thermometers, in: *Proceedings of the IEEE Sensors Conference*, Limerick, Ireland, October 28–31, 2011, pp. 1257–1260.
- [20] J.C. Salvia, R. Melamud, S.A. Chandorkar, S.F. Lord, T.W. Kenny, Real-time temperature compensation of MEMS oscillators using an integrated micro-oven and a phase-locked loop, *IEEE Journal of Microelectromechanical Systems* 19 (1) (2010 Feb) 192–201.
- [21] C.M. Jha, et al., CMOS-compatible dual-resonator MEMS temperature sensor with milli-degree accuracy, in: *Proceedings of the 14th International Solid-State Sensors, Actuators and Microsystems Conference (Transducers'07)*, Lyon, France, June 10–14, 2007, pp. 229–232.

Biographies

Igor P. Prikhodko received the BS and MS degrees (cum laude) in Mechanics and Mathematics from the Moscow State University, Moscow, Russia, in 2007, and the MS degree in Mechanical and Aerospace Engineering from the University of California, Irvine, in 2008. Currently, he is working towards the Ph.D. degree at the MicroSystems Laboratory, University of California, Irvine. His primary research focus is full-cycle research and development of inertial micromachined sensors, reflected in 5 journal and 15 refereed conference papers. He is a recipient of the 2008 Holmes Fellowship Award, the 2011 Outstanding Paper Award at the Transducers conference, and the 2012 Best Paper Award at the IMAPS Device Packaging conference. He is a member of the Institute of Electrical and Electronics Engineers (IEEE), the American Society of Mechanical Engineers (ASME), and serves as a reviewer for major MEMS journals.

Alexander A. Trusov received the BS and MS degrees in Applied Mathematics and Mechanics from the Moscow State University, Moscow, Russia, in 2004, and the M.S. and PhD degrees in Mechanical and Aerospace Engineering from the University of California, Irvine, in 2006 and 2009, respectively. He is currently a Project Scientist at the UC Irvine MicroSystems Laboratory, where he serves as a PI and Co-PI on a variety of federally sponsored programs pursuing high-performance inertial microsystems. He has published over 40 journal and conference papers on MEMS and inertial sensors, has seven pending U.S. patents, and serves as a reviewer for major journals in the fields of MEMS and sensors. His research interests include design, modeling, fabrication, and vacuum packaging of micromachined inertial systems, design of characterization experiments, and statistical data processing and analysis. He is a member of the Institute of Electrical and Electronics Engineers (IEEE) and the American Society of Mechanical Engineers (ASME). He is a recipient of an Outstanding Paper Award on low-dissipation silicon MEMS gyroscopes at the Transducers 2011 Conference.

Andrei M. Shkel received the diploma degree (With Excellence) in Mechanics and Mathematics from the Moscow State University, Moscow, Russia, in 1991, and the PhD degree in Mechanical Engineering from the University of Wisconsin, Madison, in 1997. He is a program manager in the Microsystems Technology Office of the Defense Advanced Research Projects Agency (DARPA), Arlington, VA. He is serving in this capacity while on leave from his faculty position as a professor in the Department of Mechanical and Aerospace Engineering at the University of California, Irvine, where he is also the Director of the UCI Microsystems Laboratory. He is the holder of 15 U.S. and international patents. His professional interests are reflected in more than 120 publications. He is a recipient of the 2009 Research Award from the IEEE Sensors Council, the 2006 UCI Research Award, the 2005 NSF CAREER Award, and the 2002 George E. Brown Jr., Award. He is an editor of the *Journal of Microelectromechanical Systems (JMEMS)*.